



Glycerol Trinitrate: As Potential Corrosion Protector for Mild Steel in Acid Medium Along with Paint-coated Steel in a Saline Environment

M. MENAGA*, SOWMYA RAMKUMAR and D. NALINI

Department of Chemistry, PSGR Krishnammal College for Women,
Coimbatore, Tamil Nadu, India.

*Corresponding author E-mail: mmenaga18@gmail.com

<http://dx.doi.org/10.13005/ojc/370621>

(Received: November 10, 2021; Accepted: December 18, 2021)

ABSTRACT

The importance of mild steel lies in its industrial applications, and the fight against corrosion is very important from an ecological, economic, technical, and aesthetic view. The current study involves the use of pharmaceutical drugs namely GTN towards corrosion inhibiting reaction was examined by gravimetric and electrochemical approaches. From weight loss studies, maximum I. E (%) 94.04% reached for 60 mg/L concentration of GTN for 6 h immersion time. The Polarization measurements showed that the behaviour of GTN as mixed nature and surface assimilation of GTN at the superficial, such that water molecules are substituted at the solution-metal boundary. The corrosion resistance property of the studied inhibitor as coating was also evaluated in NaCl which shows better progress corrosion retardation property of coating in the saline medium. Theoretical calculations were employed using DFT to correlate with the experimental observations.

Keywords: Mild steel, Acid corrosion, Glycerol trinitrate, Weight loss, EIS, Polarization, DFT, Epoxy resin coating.

INTRODUCTION

Mild steel has excellent mechanical properties¹ and due to this property, it is used as the material of construction engineering structural material. In petroleum industries, mild steel is extensively used transmission pipelines, dabler, flow lines, etc., where it is susceptible for oxidative degradation for which different descaling process such as acid well acidification²⁻⁵, acid cleaning, petrochemical processes are widely used for cleaning process. Mild steel undergoes corrosion

attack, due to aggressive nature⁶⁻⁸ of acidic medium. This corrosive attack can be controlled by using chemical inhibitors. Organic compounds containing N,S,O⁹⁻¹⁰ having π electron cloud are used to protect the metals and alloys¹¹ extensively and these are found to be an effective corrosion inhibitors¹²⁻¹³. The corrosion inhibitors forms productive coating, which avoids the chemical species from diffusing in mild steel ionization process. Drug play an important role as corrosion inhibitors due to i) low cost ii) easy solubility iii) biodegradability iv) less toxicity¹⁴⁻¹⁸.



The present study deals with the determination of effectiveness of GTN (Fig. 1). It is an anti-anginal drug, whose trade name is Monitgn 2.6 mg. The main constituent of the drug is glyceryl trinitrate (GTN) with the molecular formula of $C_3H_5N_3O_9$. The IUPAC name of the drug GTN is 1, 3-dinitrooxypropan-2-yl nitrate.

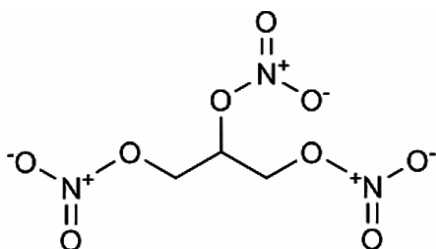


Fig. 1. Structure of corrosion inhibitor GTN

EXPERIMENTAL

Preparation of Materials

Size of mild steel specimens were cut into dimensions 5cm² exposed area for gravimetric experiments, Mild steel (Weight%: 0.098% C, 99.653% Fe, 0.02% P, 0.012% Ni, 0.201% Mn, 0.016% S and mild steel rod exposed surface area 1cm² where used for electrochemical analysis. For all the experiments the surface of the mild steel samples were polished by using a separate grade (400-1000 grit) of emery papers, then cleaned by using distilled water and dried. To prepare the corrosive medium analytical grade HCl was used with proper dilution.

Preparation of inhibitor Solution

The testing stock solution of 100 mg/L of GTN was prepared by calculated amount of powdered drug was dissolved in 1M HCl solution and the desired concentrations (5-60 mg/L) of the GTN solution are prepared by dilution the required aliquot with double distilled water.

METHODS

Weight loss method

Standard ASTM G1-03 procedure¹⁹ was applied for weight loss measurements. Properly polished and preweighed MS coupons were suspended in 100 mL of HCl solution using glass hooks without and with desired concentrations of GTN for 3 h to 24 hours. The exposed coupons were then taken out, cleaned, reweighed and the various corrosion parameters were calculated as follows.

$$IE\% = \frac{W_o - W_i}{W_o} * 100 \quad (1)$$

Where W_o and W_i specimen non-appearance and appearance the inhibitor.

$$\text{Corrosion rate (mpy)} = \frac{534 * W}{D * A * T} * 100 \quad (2)$$

$$\text{Surface Coverage } (\theta) = \frac{IE}{100} \quad (3)$$

Electrochemical measurements

Mild steel rod (1cm² area) is used working electrode, SCE as reference and Pt electrode as counter. All potentials were measured with respect to SCE. Before each measurement, OCP was calculated²⁰⁻²¹. Frequency range of EIS measurements 100 KHz to 0.01 Hz²²⁻²⁴ using 25mV amplitude. R_{ct} , C_{dl} determined from the plot Z' Vs Z'' . From the electrochemical parameters, the I. E(%) was calculated as in the formula,

$$I. E (\%) = \frac{R_{ct(y)} - R_{ct(n)}}{R_{ct(y)}} * 100 \quad (4)$$

$$IE (\%) = \frac{I_{corr(B)} - I_{corr(I)}}{I_{corr(B)}} * 100 \quad (5)$$

Where $R_{ct(y)}$, with inhibitor and $R_{ct(n)}$, without inhibitor. The corrosion current densities $I_{corr(B)}$ and $I_{corr(I)}$ for without and with different concentration in 1M HCl.

Epoxy Coating

Materials required for preparing 5ml of paint

Volume of binder-1.25 mL	Zinc -2.675 g
Volume of solvent-3 mL	Inhibitor-0.1 g
Zinc phosphate-1 g	TiO ₂ -0.4287 g

Mixed well the fine powder of TiO₂, zinc, inhibitor, zinc phosphate. A binder of epoxy resin is mixed with a hardener of polyamide. 3 mL of Xylene is used as a solvent. The mixture of epoxy resin-polyamide was added to the mixture of fine powder grained well and solvent was added drop by drop until a paint form is obtained and painted on mild steel which are was labelled as A, B and C. A-bare mild steel specimen without epoxy coating, B-Mild steel with epoxy coating (2mm thickness), C-Mild steel with epoxy coating containing GTN(2mm thickness).The coated coupons dried at 78 h and studied in 3.5% NaCl.

Electrochemical Measurements of the paint coating mild steel

Electrochemical measurements were carried out in a similar setup of three electrode system using the epoxy coated coupons as working electrode in saline environment.

Theoretical methods

The inhibitor geometrical structure was optimized completely with the program package GAUSSIAN 09 followed by B3LYP procedure²⁵⁻²⁷ within the basic set of 6-31G²⁸. All the quantum chemical parameters of electronegativity (χ), dipole moment (μ), global hardness (η), E_{LUMO} , E_{HOMO} , Global softness (σ), ΔE , ΔN were discussed for the studied compound.

RESULTS AND DISCUSSION

Gravimetric measurements

Based on gravimetric investigation on mild steel specimen, the stability of the inhibitor molecules was evaluated. The measurements obtained after 3 h, 6 h, 12 h and 24 h immersion time at 298K with

different concentration of GTN (5-60 mg/L) was clearly predicted in Table 1. Thus as the inhibitor GTN concentration increases there is a increase in the I. E (%)²⁹⁻³³ and corrosion rates decreases. The result shows that the metal surface are blocked by the GTN inhibitor molecules from the corrosion solution. After 6 h of immersion, I. E (91.01%) was found to decrease which may be attributed³⁴⁻³⁸. Metal due to prologed exposure of metal to the medium. With increased immersion time upto 24 h there is found to be an increase in the corrosion rate³⁹⁻⁴². This result can be explained by the theory of adsorption. GTN molecules were desorbed, on prolonged immersion on the mild steel specimen surface, thereby increases the surface corrosive environment interaction. Moreover, the corrosion rate increases with increasing contact time, which was assigned to a small amount of GTN molecules being adsorbed in the surface to control the metal dissolution process. Hence it is clear that after 6 h of immersion time, GTN molecules were desorbed, they turned to be ineffective as they are not involve in the inhibitive process.

Table 1. The inhibition of GTN from Gravimetric measurements

Conc mg/L	3 h		6 h		12 h		24 h	
	CR mm/y	IE %	CR mm/y	IE %	CR mm/y	IE %	CR mm/y	IE %
Blank	1168	-	1351	-	3279	-	6491	-
5	601	48.53	422	68.73	1073	67.27	3378	47.95
10	548	53.06	296	78.04	1038	68.32	3316	48.91
15	492	57.82	186	86.18	714	78.22	2783	57.11
20	447	61.68	168	87.55	671	79.52	2526	61.07
25	408	65.08	151	88.82	592	81.94	2043	68.52
30	374	67.91	147	89.12	597	81.78	1910	70.57
35	307	73.7	143	89.41	551	83.19	1737	73.24
40	282	75.85	137	89.8	536	83.64	1722	73.46
45	231	80.16	131	90.29	477	85.45	1710	73.65
50	201	82.77	128	93.16	378	88.44	1657	74.46
55	169	85.49	124	93.78	314	90.42	1603	75.30
60	139	88.10	94	94.04	291	91.11	1462	77.46

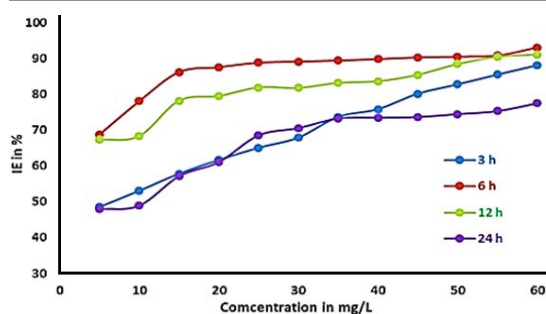


Fig. 2. Influence of various concentrations on the I.E of GTN for mildsteel in 1M HCl

Effect of the inhibitor concentration on protection ability over time is presented in Fig. 2. It was clear from figure that at lower immersion time (3 h) there was a steady increase in the inhibition efficiency with concentration but for higher immersion time (6 & 12 h) the efficiency of the inhibitor GTN increases upto 15 mg/L concentration after which there is not much pronounced effect in its corrosion inhibiting performance. Thus optimal concentration of GTN attaining the maximum efficiency at 15 mg/L in 1M HCl.

Potentiodynamic polarization measurements

At different concentration, the electrochemical reaction potential and current were determined from the point intersection of cathodic and anodic curves by extrapolation of linear parts of the Tafel plots. As evidenced from the Tafel plot (Fig. 3) GTN affects both bc and ba. It is also proved from the change in both the tafel slopes values

which proves that GTN inhibitor behaves with mixed nature. I.E(%), it reaches maximum efficiency 85.7% at 60 mg/L (Table 2). This results indicates that the GTN inhibitor, surface of the metal active sites are blocked and formed by a barrier between the charge transfer and mass which are the evidences for the decrease in the interaction of the metal surface with the corrosive environment.

Table 2: Polarization parameters for the corrosion of mild steel without and with various concentrations of GTN in 1M HCl

Concentration mg/L	E_{corr} mV	I_{corr} $\mu\text{A}/\text{cm}^2$	IE%	bc mV/dec	ba mV/dec	R_p $\Omega \text{ cm}^2$	IE%
Blank	-543	217	-	101	117	108	-
5	-525	130	40.09	76	146	166	34.94
15	-525	75	65.44	91	136	314	65.61
30	-529	54	75.12	86	139	430	74.88
45	-529	45	79.26	81	135	469	76.97
60	-529	31	85.71	82	137	492	78.05

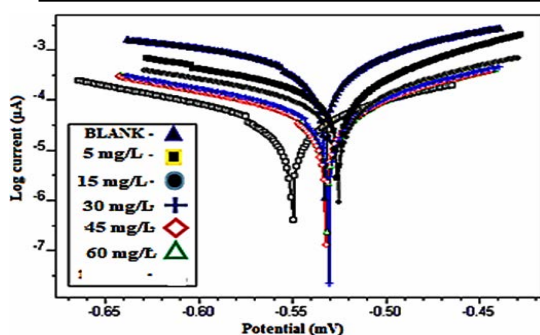


Fig. 3. Polarization curves observed for mild steel electrode in 1M HCl including addition concentrations of GTN

Electrochemical impedance spectroscopic measurements

From Fig. 4 and Table 3, the experimental curves are best fit and the electrochemical parameters are obtained. The results shows that as inhibitor concentration increases there is an increase in the R_p and decreases in C_{dl} . R_p values are increases with inhibitor concentration designates growth in the θ , causing the inhibition efficiency increases.

Table 3: EIS parameters for mild steel in HCl with GTN

Concentration mg/L	R_s $\Omega \text{ cm}^2$	R_{ct} $\Omega \text{ cm}^2$	IE %	C_{dl} $\mu\text{F}/\text{cm}^2$	θ
Blank	6.81	19	-	12.9	-
5	9.23	45	58.04	26.4	-1.0465
15	16.6	68	72.42	23	-1.0465
30	16.1	107	82.4	19.1	-0.7829
45	19.2	114	83.39	18.2	-0.4806
60	20.3	135	86.03	17.5	-0.4109

Because the adsorption of the inhibitor molecule increases with increased concentration,

the C_{dl} value lowers, indicating that the contact of the metal surface area with the medium reduces. The interface layer is affected by the increased substitution of water at the solution-metal border, which decreases the dielectric constant value. The shift in the C_{dl} value, which corresponds to the decrease in the amount of the metal deterioration, is a proof for the displacement of water at the interface double layer. The superficial heterogeneity is represented by constant n values. The n rate increases, indicating that the surface of mild steel becomes more and more homogeneous as the inhibitor concentration rises due to the increased surface coverage.

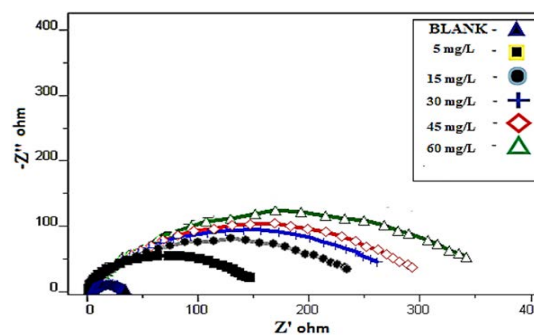


Fig. 4. Nyquist plots for mild steel corrosion in 1M HCl without and with GTN Concentrations

Epoxy coating behavior of GTN in 3.5% of NaCl

Fig. 5 depicts an equivalent circuit model of the cell system. It was used to fit curves and determine the resistance and coating capacitance of epoxy coating systems. R_t —charge transfer resistance, CPE_{coat} —coating capacitance, R_s —solution resistance, R_{coat} —coating resistance, CPE_{dl} —double layer capacitance.

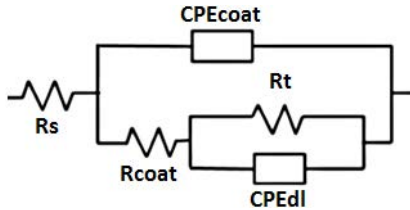


Fig. 5. Combining the EIS data with the Equivalent circuit model

From the Fig. 6 Nyquist plot for the coating in 3.5 percent NaCl was investigated. The coatings investigated show a larger capacitive loop in the Nyquist plots at first, with the dielectric response matching that of the coating⁵²⁻⁵³. The coating acts as a barrier layer and has a high coating resistance (R_{coat})⁵⁴. The impedance spectroscopy shows only one gradually diminished capacitive arc after a few hours of immersion, indicating ongoing penetration of the electrolyte solution and little electrochemical processes. In addition, the coating's macroscopic appearance remains unaffected. Because the mass transfer pcorrosion mechnaism is impeded in presence of GTN, a diffusion tail forms in the impedance spectroscopy as the immersion time increases.

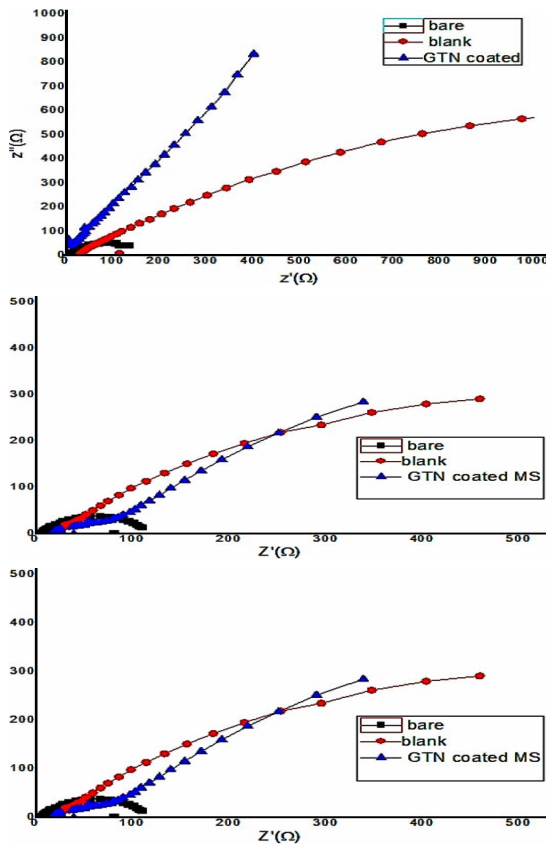


Fig. 6. Nyquist plot of epoxy coated mild steel coupons in NaCl (a) 0 h, (b) 48 h and (c) 168 hours

Potentiodynamic polarization studies in 3.5% of NaCl

As illustrated in Fig. 7, the potentiodynamic polarization plots reveal the favourable effect of paint coating when compared to bare MS (A), epoxy coated MS (B), and epoxy coated MS including the inhibitor (C) in a saline environment. The electrochemical characteristics of the corrosion process, E_{corr} , I_{corr} , b_a & b_c are given in Table. 5 shown. (b_a , b_c). The corrosion potentials on painted mild steel surfaces moved to lower negative values, and the anodic current densities on these surfaces were lower than on polished mild steel surfaces⁵⁵. These findings can be taken as demonstrating that an epoxy-coated steel surface is more corrosion resistant than an untreated steel surface. This study demonstrates a significant improvement in corrosion resistance coating. The resistance was determined to be low on the seventh day.

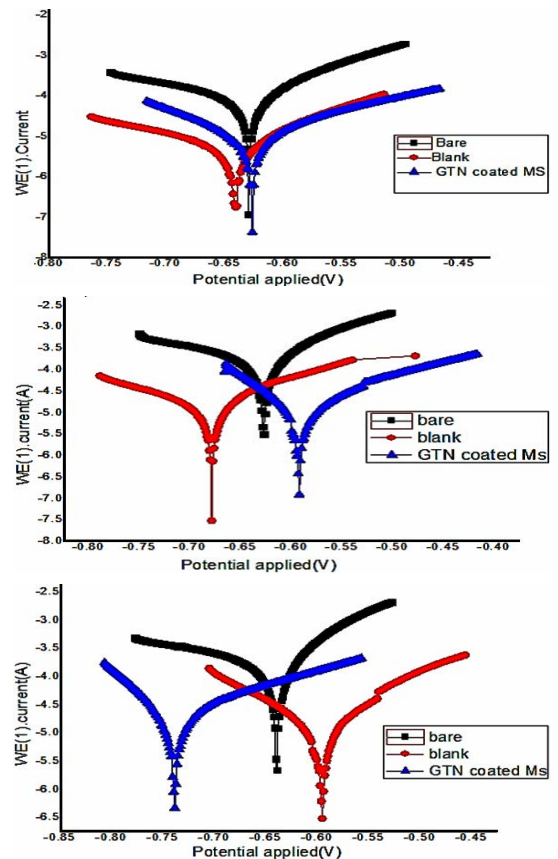


Fig. 7. Tafel plot of painted coupons in NaCl (3.5%) at (a) 0 h (b) 48 h (c) 168 hours

Table 4: Electrochemical impedance characteristics for paint coated mild steel corrosion in NaCl

Sample Name	Ageing period (hours)	R_s (Ω cm ²)	C_{dl} (mF/cm ²)	R_{coat} (Ω cm ²)	R_t (Ω cm ²)	R_{tot} (Ω cm ²)
Bare Mild Steel	0	8.1	9×10^{-7}	3922	-3849	73
	48	7.3	9×10^{-7}	-8.54	7.4	-1.1
	168	9.6	1.13×10^{-5}	-31.4	29	-60.4
Epoxy coated mild steel	0	22.2	132	939	151	1090
	48	26.4	9×10^{-7}	804	-7535	499
	168	33.8	9×10^{-7}	-176	168	-8
Epoxy coated mild steel with GTN	0	58	118	1830	285	2115
	48	48	571	1217	98	1315
	168	59	9×10^{-7}	-5665	6012	347

Table 5: Parameters of potentiodynamic epoxy coated coupons in NaCl (3.5%)

Sample	Ageing period (hours)	E_{corr} (mV)	I_{corr} (μ A/cm ²)	ba (mV/dec)	bc (mV/dec)
A	0	-634	190	481	126
	48	-647	9.92	299	118
	168	-638	16	142	161
B	0	-647	9.92	299	118
	48	-693	66	122	287
	168	-595	21	155	121
C	0	-638	16	142	161
	48	-608	18	9	155
	168	-738	27	84	208

Quantum chemical Studies

Frontier molecular orbitals (HOMO, LUMO) is the calculation form of quantum chemical studies. It is used to relate the inhibition efficiency and the molecular structure of the inhibitor⁵⁶⁻⁵⁹. Fig. 8 represents the charge distribution of the GTN inhibitor. The electron donating and electron accepting ability is related to energies of frontier molecular orbitals in a molecule. Fig. 9a & b represents the E_{HOMO} and E_{LUMO} of the inhibitor molecule.

From Table 6, quantum chemistry parameters that are arrangement molecules' well-known minimal energy configuration. High E_{HOMO} values⁶⁰ indicate a molecule that has a proclivity for donating electrons to the Fe atom's vacant d orbital⁶¹⁻⁶². The high value of HOMO, -11.99 eV, and the very low value of LUMO, -1.80 eV, corresponding to the value of E (10.19 eV), have an insignificant value, indicating that the energy required for electron elimination, resulting in good inhibition efficiencies and a better dipole moment. The dipole value of 4.677eV indicates that the investigated inhibitor system has good adsorption characteristics on the metal surface.

Global hardness η are important pointer of a molecules tendency concerning covalent

interaction, softness are accelerate the surface and molecules interaction as well as the metal state and hybridization⁶³. From Table 6 visibly η have lower values (5.09eV) that indicates the high corrosion inhibition potential of GTN. Global softness (σ) is 0.09eV. According to Lukovis *et al.*, a N value of less than 3.6 implies that GTN has a stronger potential to donate electrons⁶⁴. The electron-donating capacity of GTN is confirmed by the same order of N and E_{HOMO} .

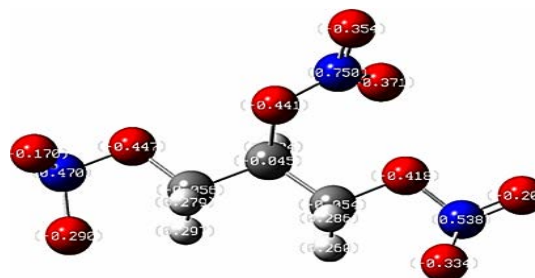


Fig. 8. Charge distribution structure of GTN

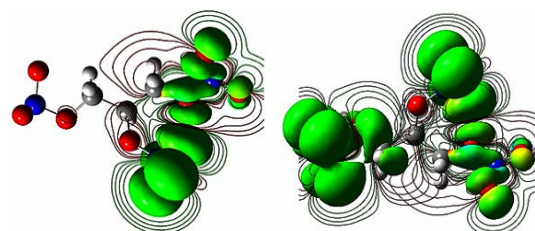


Fig. 9(a). The GTN's HOMO

Fig. 9(b). The GTN's LUMO

Table 6: Quantum chemical parameters obtained by DFT calculation

Quantum chemical Parameters	GTN
Molecular Formula	C ₃ H ₅ N ₃ O ₉
Total Energy (a.u)	-947.36
E _{HOMO} (eV)	-11.99
E _{LUMO} (eV)	-1.80
ΔE (eV)	10.19
Dipole Moment (μ) (eV)	4.677
Global Hardness (η) (eV)	5.09
Global Softness (σ) (eV)	0.09
Electronegativity (χ) (eV)	6.89
ΔN	0.1

CONCLUSION

The inhibitive nature of a pharmaceutically active chemical, glyceryl trinitrate GTN, against acid corrosion and as an epoxy coating protection in a salty environment was investigated using the following data.

In 1M HCl, the pharmaceutically active chemical glyceryl trinitrate GTN inhibited mild steel corrosion, and notable efficiency increase when noted for incremental change in inhibitor concentration.

The inhibitive action was attributed to the inhibitor molecule after becoming physically

adsorbed. The Langmuir isotherm governs the adsorption process.

The mixed type nature of GTN in acid media is demonstrated by its polarisation behaviour.

Impedance studies of paint coating in 3.5 percent NaCl demonstrate that including GTN into the paint improves the performance of the coating, resulting in a coating with strong antipermeability resistance. It's also worth noting that, thanks to these new refined passivation methods, the produced epoxy coatings with GTN might save the a lot money.

Inhibitive impact examined substances was connected with data derived from DFT calculation. Both experimental and theoretical calculations coincide well.

ACKNOWLEDGEMENT

The authors express their gratitude to PSGR Krishnammal College for Women, DST-FIST, UGC, for the financial support providing the essential facilities.

Conflict of interest

There are no conflicts of interest declared by any of the authors.

REFERENCES

1. Veedu, K.K.; Kalarikkal, T. P.; Jayakumar, N.; Gopalan, N. K.; *ACS Omega*, **2019**, *4*, 10176–10184.
2. Sowmya Ramkumar.; Mumtaz, Nalini, D.; Eno, A. Q.; *J. Heterocycl. Chem.*, **2019**, *1–17*
3. Mohan, R.; Joseph, A.; *Egypt. J. Pet.*, **2018**, *27*, 11–20.
4. Liao, L. L.; Mo, S.; Luo, H. Q.; Feng, Y. J.; Yin, H. Y.; Li, N. B.; *Corros. Sci.*, **2017**, *124*, 167–177.
5. Ouknin, M.; Romane, A.; Ponthiaux, J.; Costa, J.; *J of Corrosion reviews.*, **2020**, *38*.
6. Ben, M.; Abubshait, S.; Etteyeb, N.; Kamoun, M.; *Arab. J. Chem.*, **2020**, *13*, 4846–4856,
7. Mobin, M.; Zehra, S.; Aslam, R.; *RSC Adv.*, **2016**, *6*, 5890–5902.
8. Nwankwo, H. U.; Olasunkanmi, L. O.; Ebenso, E. E.; *Sci. Rep.*, **2017**, *7*, 2436.
9. K. Azzaoui K.; *Corros. Sci.*, **2017**, *129*, 70–81, 2017.
10. Zheng, X.; Zhang, S.; Gong, M.; Li, W.; *Ind. Eng. Chem. Res.*, **2014**, *53*, 16349–16358.
11. Bendaif, H.; Melhaoui, A.; AzzouziM, El.; Legssyer, B; Hamat, T; Elyoussf, A.; Aouniti, AE.; Ouadi, Y.; Aziz, M.; *J Mater Environ Sci.*, **2016**, *7*, 1276–1287.
12. Verma, C.; Olasunkanmi, LO.; Ebenso, EE.; Quraishi, MA.; Obot, IB.; *J Phys Chem C.*, **2016**, *120*, 11598–11611.
13. Verma, C.; Olasunkanmi, OIB.; Ebenso, EE.; Quraishi, MA.; *RSC Adv.*, **2016**, *6*, 1–50.
14. Alan Miralrio, Araceli Espinoza Vázquez A.; *J of Process.*, **2020**, *8*, 942.
15. Fouda, A.S.; Ibrahim, H.; Rashwaan, S.; Ahmed, R. M.; **2018**, *13*, 6327–6346.
16. As, F.; Ma, E. M.; El, T., **2017**, *5*, 1–8.
17. Abeng F. E.; Valentine, A.C., **2020**.
18. Diki, N.; Silvére, Y.; Valery, B.K.; Guy-richard, M.; Augustin, O., **2018**, *11*, 24–36.
19. ASTM G1-03, "Standard practice for preparing, cleaning and evaluating corrosion test specimens", ASTM International, West Conshohocken, USA., **2003**.

20. Gurudatt, D.M.; Mohana, K.N.; *Ind. Eng. Chem. Res.*, **2014**, 53, 2092–2105.
21. A. E. S. Fouda, A.E.S.; El-maksoud, S. A. A.; El-sayed, E.H., **2021**, 13497–13512.
22. Mirzakhazadeh, Z.; Kosari, A.; Moayed, M.H.; Naderi, R.; Taheri, P.; Mol, J. M. C.; *Corros. Sci.*, **2018**, 138, 372–379.
23. Mishra, A.; Verma, C.; Lgaz, H.; Srivastava, V.; Quraishi, M.A.; Ebenso, E. E.; *J. Mol. Liq.*, **2018**, 251, 317–332.
24. Ansari, K. R.; Quraishi, M. A.; Singh, A.; Ramkumar, S.; Obote, I. B.; *RSC Adv.*, **2016**, 6, 24130–24141.
25. Abdallah, M.; El Defrawy, A.M.; Zaafarany, I.A.; Sobhi, M.; Elwahy, A.H.M.; Shaaban, M.R.; *Int. J. Electrochem. Sci.*, **2014**, 9, 2186–2207.
26. Kathirvel, K.; Thirumalairaj, B.; Jaganathan, M.; *Open J. Met.*, **2014**, 04, 73–85.
27. Momeni, M.J.; Behzadi, H.; Roonasi, P.; Sadjadi, S.A.S.; Mousavi-Khoshdel, S.M.; Mousavi, S.V.; *Res. Chem. Intermed.*, **2015**, 41, 6789–6802.
28. Ansari, K.R.; Quraishi, M.A.; Singh, A.; Sowmya Ramkumar; Obote, I.B.; *RSC Adv.*, **2016**, 6, 24130–24141.
29. Li, X.; *Arab. J. Chem.*, **2014**.
30. Prabhu, R. A.; Venkatesha, T. V.; Praveen, B. M.; Chandrappa, K. G.; Hamid, S. B. A.; **2014**, 67, 675–679.
31. Gaaz, T.S.; Takriff, M.S.; **2020**, 1–8.
32. Abeng, F. E.; Anadebe, V.C.; Nkom, P. Y.; Uwakwe, K. J.; Kamalu, E. G.; **2021**, 11, 11–26.
33. Ogunleye O. O.; Arinkoola, A. O.; Eletta O.O.; Agbede, Y.A.Osho.; Morakinyo.A.F.; Hamed, J. O., **2020**, 6, e03205.
34. Tourabi, M.; Nohair, K.; Nyassi, A.; Hammouti, B.; Jama, C.; Bentiss, F.; *J. Mater. Environ. Sci.*, **2014**, 5, 1133–1143.
35. Bammou, L.; Belkhaouda, M.; Salghi, R.; Benali O.; Zarrouk, A.; Al-Deyab, S. S.; Warad, I.; Zarrok, H.; Hammouti, B.; *Int. J. Electrochem. Sci.*, **2014**, 9, 1506–1521.
36. Iroha N.B.; Nnanna, L.A., **2019**, 10, 898–908.
37. Fouda, A. S.; Hassan, A. F.; Elmorsi, M. A.; Fayed, T. A.; Abdelhakim, A.; *Int. J. Electrochem. Sci.*, **2014**, 9, 1298–1320.
38. Kosari, A.; Moayed, M.H.; Davoodi, A.; Parvizi, R.; Momeni, M.; Eshghi, H.; Moradi, H.; *Corros. Sci.*, **2014**, 78, 138–150.
39. Hameed, R. S. A.; Al, E. A. I. H. I.; Mohamed, S.; *J. Bio-Tribo-Corrosion.*, **2020**, 1-10.
40. Arockiasamy, P.; Sheela, X. Q. R.; Thenmozhi, G.; Franco, M.; Sahayaraj, J. W.; Santhi, R.J.; *International Journal of Corrosion.*, **2014**,
41. Ahmed, R. A.; Farghali, A.; Fekry, A.M.; *Int. J. Electrochem. Sci.*, **2012**, 7, 7270–7282.
42. Zaafarany, I. A.; Hamza A. Ghulman, *Int. J. Corros.*, **2013**, 2, 82-161.
43. Ansari, K.R.; Sowmya Ramkumar.; Nalini, D.; Quraishi, M. A.; *Cogent.*, **2016**, 2, 1145032.
44. Seikh A. H.; Sherif, E. M.; **2015**, 10, 895–908,
45. Taylor, P.; Ghasemi, O.; Danaee, I.; Rashed, G.R.; Avei, M. R.; Maddahy, M. H., **2015**, 37–41.
46. Khelifa, A.; Hamitouche, H.; Khadraoui, A.; Hadj Ziane, A.; *J. Mater. Environ. Sci.*, **2015**, 6, 1890–1895.
47. Khadiri, A.; Saddik, R.; Bekkouche, K.; Aouniti, A.; Hammouti, B.; Benchat, N.; *J. Taiwan Inst. Chem. Eng.*, **2015**, 100, 1–13.
48. Sowmya Ramkumar., Nalini, D.; *Mater. Today Proc.*, **2019**, 18, 1696–1708.
49. Hamdan, A.B.; Suryanto.; Haider, F.I.; *J. Mater. Environ. Sci.*, **2014**, 5, 767–778.
50. Barba, V.; Ríos, J. P. F. L., Casales, M., **2021**.
51. K. R. Ansari, K. R.; Sowmya Ramkumar, S.; D. Nalini, D.; and M. A. Quraishi, M.A.; *Cogent Chem.*, **2016**, 2.
52. Qi, K.; Sun, Y.; Duan, H.; Guo, X.; *Corros. Sci.*, **2015**, 98, 500–506.
53. Sowmya Ramkumar.; Nalini, D.; *Orient. J. Chem.*, **2015**, 31, 1057-1064.
54. Z. Chen, Z.; C. He, C.; F. Yu, F.; Wang, Y.; **2017**, 12, 2798–2812.
55. Rajasekharan, V.; Stalin, T.; Viswanathan, S.; Manisankar, P.; **2013**, 8, 11327-11336.
56. Hadisaputra, S.; Hamdiani, S.; Purwoko, A.A.; *J. Appl. Chem. Sci.*, **2017**, 312–317.
57. Sowmya Ramkumar.; Nalini, D.; *Orient. J. Chem.*, **2015**, 31, 1057-1064.
58. Al-amiry, A.; Salman, T. A.; Alazawi, K. F.; Shaker, L. M.; Kadhum, A.A.H.; Takriff, M. S.; **2020**, 202–209.
59. Eldesoky, A. M.; Diab, M. A., El-Bindary, A. A.; El-Sonbati, A. Z.; Seyam, H. A.; *J. Mater. Environ. Sci.*, **2015**, 6, 2148–2165.
60. Sowmya Ramkumar.; Nalini, D.; *Orient. J. Chem.*, **2015**, 31, 1057-1064.
61. A. Mishra A.; Ankusg Mishra.; Chandrabhan verma.; Srivastava, V.; Lgaz, H.; Quraishi, M. A.; Eno. E. Ebenso., *J. Bio- Tribo-Corrosion.*, **2018**, 4, 0.
62. Junaedi, S.; Al-Amiry, A.A.; Kadhum, A.; Kadhum, A. A. H.; Mohamad, A. B.; *Int. J. Mol. Sci.*, **2013**, 14, 11915–11928.
63. Ansari, K.R.; Quraishi, M. A.; Ambrish singh.; Sowmya Ramkumar.; Obote, B.; *RSC Advances.*, **2016**, 6, 24130-24141.
64. Zohdy, K. M.; Rabab, M.; El-Sherif, Sowmya Ramkumar, El-Shamy, A. M.; *EL Upstream Oil and Gas Technology.*, **2021**, 6,